

Stationary Growth and Unique Invariant Harmonic Measure of Cylindrical Diffusion Limited Aggregation

Riccardo Marchetti,¹ Alessandro Taloni,^{1,2} Emanuele Caglioti,³ Vittorio Loreto,^{1,4} and Luciano Pietronero^{1,5}

¹*Dipartimento di Fisica, La Sapienza Università di Roma, P.le A. Moro 5, 00185 Rome, Italy*

²*CNR-IENI, Via R. Cozzi 53, 20125 Milano, Italy*

³*Dipartimento di Matematica, La Sapienza Università di Roma, P.le A. Moro 5, 00185 Rome, Italy*

⁴*ISI Foundation, Via Alassio 11/c 10126 Torino, Italy*

⁵*CNR-ISC, Via dei Taurini 19, 00185 Rome, Italy*

(Received 28 March 2012; published 8 August 2012)

We prove that the harmonic measure is stationary, unique, and invariant on the interface of diffusion limited aggregation (DLA) growing on a cylinder surface. We provide a detailed theoretical analysis puzzling together multiscaling, multifractality, and conformal invariance, supported by extensive numerical simulations of clusters built using conformal mappings and on a lattice. The growth properties of the active and frozen zones are clearly elucidated. We show that the unique scaling exponent characterizing the stationary growth is the DLA fractal dimension.

DOI: [10.1103/PhysRevLett.109.065501](https://doi.org/10.1103/PhysRevLett.109.065501)

PACS numbers: 61.43.Hv

Introduction.—Albeit the diffusion limited aggregation model (DLA) was introduced 30 years ago [1], it still embodies the perfect puzzle for theorists. In spite of the enormous amount of numerical works, only few rigorous results are proven, and these all concern the generalized dimensions of the aggregate. The notion of varying dimensionality characterizes the DLA growth in two ways: multiscaling and multifractality. Multiscaling suggests that the aggregate's fractal dimension attains different local values $d(r/R)$ on each circular ring of radius r , while the overall gyration radius $R(N) \sim N^{1/D}$ (N and D , cluster's particles number and fractal dimension) [2,3]. Multifractality [4] entails the introduction of generalized dimensions $D(q)$, which correspond to the fractal dimension of the q points correlation function. The aforementioned rigorous results are: $D(0) \geq 3/2$ [5], $D(1) = 1$ [6] and $D(3) = D(0)/2$ [7]. A simpler definition of $D(q)$ is provided by the connection with the harmonic measure, i.e., the growth probability at the interface. In general, the determination of the harmonic measure within the fjords of the fractal, is a quite impossible task if resorting to the usual numerical techniques [8]. Iterated conformal mapping [9] provides a solution to this problem [10]: indeed, it is based on the representation of the growth dynamics via the convolution of elementary complex functions $\phi_{\lambda_n, \theta_n}(w)$, hereafter, named $\phi_n(w)$, which map the unitary circle onto a unitary circle with a bump of linear size $\sqrt{\lambda_n}$ placed at position $w = e^{i\theta_n}$ [11]. The ensuing function $z = \Phi^{(N)}(e^{i\vartheta}) = \phi_1 \circ \phi_2 \circ \dots \circ \phi_N(e^{i\vartheta})$ transforms the unitary circle $e^{i\vartheta}$ onto the cluster's interface z . Furthermore, conformal mapping has been extended to DLA growing on a cylinder surface [12]: in this case, the mapping function is

$$\Xi^{(N)}(e^{i\vartheta}) = -i \frac{L}{2\pi} \ln[\Phi^{(N)}(e^{i\vartheta})], \quad (1)$$

where L is the cylinder circumference and $\Phi^{(N)}$ represents the radial deformation of the cylindrical aggregate (see Supplemental Material [13]). The DLA overall height grows as $h(N) \simeq \frac{L}{2\pi} \ln F_1^{(N)}$, where $F_1^{(N)} = \prod_{n=1}^N \sqrt{1 + \lambda_n}$ is the first Laurent coefficient of $\Phi^{(N)}$ [9,11].

In this Letter, we provide another rigorous result concerning the harmonic measure of a DLA growing in a cylindrical geometry. We show that the growth probability at the interface is stationary, unique, and invariant, leading to the conformal invariance of the complex mapping function. Our framework provides the natural connection between multiscaling and multifractality, and offers a clear-cut definition of the frozen and active zone of the aggregate. Moreover, we show that the stationarity leads to the appearance of the fractal dimension D as the unique exponent governing the growth dynamics, in striking contrast to DLA in radial geometry.

Height's scaling and growth velocity.—The average height of a cylindrical aggregate grows according to the following law [12]: $\langle h(N) \rangle = L \left(\frac{N}{\langle n_0 \rangle}\right)^\beta$ if $N \ll \langle n_0 \rangle$ and $\langle h(N) \rangle = L \frac{N}{\langle n_0 \rangle}$ if $N \gg \langle n_0 \rangle$ [$\beta \simeq 4/3$, $\langle n_0 \rangle = \frac{1}{\pi} (\frac{\sqrt{\lambda_0}}{L})^{-D}$] (Ref. [13], Fig. 7). The first regime accounts for a self-affine initial growth, while the DLA attains the linear self-similar regime after an average time $\langle n_0 \rangle$, namely, the transient on which the cluster forgets about its initial condition, i.e., the cylinder's baseline. From the scaling of $\langle h(N) \rangle$ and the expression of $F_1^{(N)}$, one obtains $\langle h(N) \rangle \simeq \frac{L}{4\pi} \sum_{n=1}^N \langle \lambda_n \rangle$, which furnishes the expression of the average height's growth velocity: $d\langle h(N) \rangle/dN \simeq \frac{L}{4\pi} \langle \lambda_N \rangle$. Thus, the average elementary increment $\langle \lambda_n \rangle$ grows as $\sim 4\pi\beta \frac{n^{\beta-1}}{\langle n_0 \rangle^\beta}$ for $n \ll \langle n_0 \rangle$, and it gets to the stationary value $\frac{4\pi}{\langle n_0 \rangle}$ for $n \gg \langle n_0 \rangle$ (Ref. [13], Fig. 8). This suggests that self-similarity is intimately connected to the height's velocity

stationary growth, in contrast with DLA in radial geometry [11]: in this case, the radius growth is clearly nonstationary and $\langle \lambda_n \rangle = 2/(nD_R)$, with $D_R \approx 1.71$ radial cluster's dimension.

Harmonic measure.—We now proceed to the evaluation of the harmonic measure [1]. The DLA interface is the union of different arcs, which are the (remaining) boundaries of the N particles composing the cluster. Each arc may be labeled by Δz_n where n is the generation when the n -th bump was added to the structure; besides, we identify the middle point z_n as the representative point of the entire arc [Fig. 2, inset (b)], and we calculate the probability $P^{(N)}(z_n)$. The latter is the normalized electric field on the fractal's interface [14], i.e., $P^{(N)}(z_n) \propto |E^{(N)}(z_n)|$, which is connected to the Jacobian of Eq. (1) as $|E^{(N)}(z_n)| = |\nabla \Xi^{(N)}(e^{i\vartheta_n^N})|^{-1}$ [9,11]. The angle ϑ_n^N represents the counterimage of z_n on the unitary circle, and must be subjected to a reparametrization whenever a new particle is added [10,12]. Indeed consider a DLA at two different generations N and $N - k$, with $k \in [1, N - n]$: the position z_n remains unchanged whether the cluster has N or $N - k$ particles, i.e., $z_n = \Xi^{(N)}(e^{i\vartheta_n^N}) = \Xi^{(N-k)}(e^{i\vartheta_n^{N-k}})$, yielding

$$e^{i\vartheta_n^N} = \phi_N^{-1} \circ \phi_{N-1}^{-1} \circ \dots \circ \phi_{N-k+1}^{-1}(e^{i\vartheta_n^{N-k}}), \quad (2)$$

where ϕ_n^{-1} is the inverse of ϕ_n [10,12]. Thus, any ϑ_n^N can be determined from its initial value $\vartheta_n^N \simeq \theta_n$. The electric field at z_n can be calculated as $|E^{(N)}(z_n)| = \frac{|E^{(n)}(z_n)|}{\prod_{k=n+1}^N |\phi'_k(e^{i\vartheta_k^k})|}$, where ϕ'_n is the derivative of ϕ_n . Figure 1 shows the probability $P^{(N)}(z_n)$ as a function of n , for a single DLA realization at six different values of N . The harmonic measure $\mu_{N,n}$ is the ensemble average of $P^{(N)}(z_n)$, i.e., $\mu_{N,n}(\frac{\sqrt{\lambda_0}}{L}) = \langle P^{(N)}(z_n) \rangle$; from the numerics its behavior is stationary, depending solely on the difference $N - n$:

$$\mu_{N,n} \simeq \frac{1}{\langle n_p \rangle} \times \begin{cases} \left(\frac{n}{\langle n_p \rangle}\right)^\beta e^{-(N-n/\langle n_p \rangle)} & n \ll \langle n_0 \rangle \\ e^{-(N-n/\langle n_p \rangle)} & \langle n_0 \rangle \ll n \ll N - \langle n_{AZ} \rangle, \\ \left(\frac{\sqrt{\lambda_0}}{L}\right)^{\alpha(n-N/\langle n_p \rangle)} & N - \langle n_{AZ} \rangle \ll n \ll N \end{cases} \quad (3)$$

n_{AZ} represents the number of particles that compose the active zone of the DLA [15]. Firstly, we focus on the frozen zone for which $n \ll N - \langle n_{AZ} \rangle$: a quantitative analysis of the measure's scaling in the active region, will be given in the following. The probability of a point belonging to the frozen interface exhibits an apparent exponential decay, with a characteristic time n_p . This arises from the electric field expression, indeed for any point in the frozen zone $|\phi'_k(e^{i\vartheta_k^k})| \simeq e^{1/n_p}$, if $k \gg n + n_{AZ}$. This suggests that a point in the frozen zone cannot influence the growth dynamics, since the probability in z_n does not depend on the specific choice of the elementary function ϕ_k when $k \gg n + n_{AZ}$. On the other side, it points to the notion of

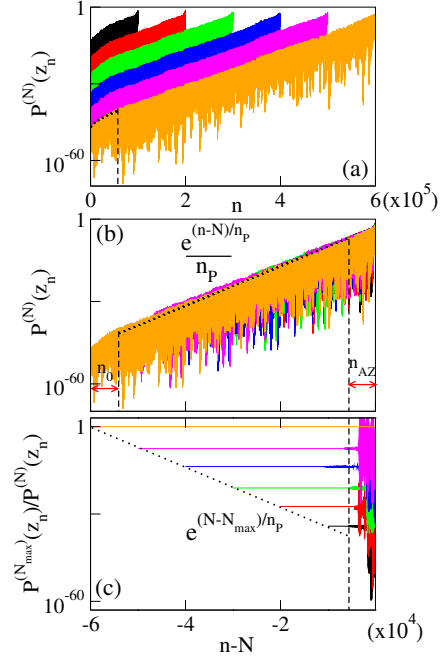


FIG. 1 (color online). Probability distribution on DLA interface. $P^{(N)}(z_n)$ is shown for a single DLA realization ($\lambda_0 = 10^{-5}$, $L = 1$) for $N = 10^4, 2 \times 10^4, 3 \times 10^4, 4 \times 10^4, 5 \times 10^4$ and 6×10^4 (from left to right). (a) $P^{(N)}(z_n)$ as function of generation n : dotted line corresponds to the self-affine regime, i.e., $\frac{n^\beta}{n_p^{\beta+1}} e^{-(N-n/n_p)}$ ($\beta = 4/3$). (b) Rescaling of $P^{(N)}(z_n)$: probabilities at different N collapse on top of each other exhibiting the $N - n$ dependence. Dashed lines show the self-affine region (n_0) and the active zone (n_{AZ}). (c) Ratio between $P^{(N_{\max})}(z_n)$ ($N_{\max} = 6 \times 10^4$) and the curves in panel (a), showing the stationarity in the frozen zone (from bottom to top).

conformal invariance [9], since two conformal transformations ϕ_n and ϕ_k commute whenever $k \gg n + n_{AZ}$. Indeed, given a mapping function $\Xi^N(w)$ with $N - n_{AZ} \gg k \gg n + n_{AZ}$, the size of the new bump $\sqrt{\lambda_{N+1}}$ and the ensuing growth dynamics will remain unchanged whether ϕ_k is swapped with ϕ_n . n_p can be accurately measured for any z_n lying in the frozen zone, indeed from Eq. (3) one has $n_p = (N_2 - N_1)/[\ln P^{(N_1)}(z_n) - \ln P^{(N_2)}(z_n)]$, with N_2 and N_1 two arbitrary generations. The scaling of $\langle n_p \rangle$ is displayed in Fig. 3.

Active zone.—A zoom of $\mu_{N,n}$ for $n \in [N - \langle n_{AZ} \rangle, N]$ is shown in Ref. [13] in Fig. 9 panel (a). The active zone is the region where new particles join the existing cluster [15–17]; our observation indicates that it corresponds to the region occupied by the last n_{AZ} (Fig. 2). Conformal mapping transforms $\mu_{N,n}$ to the uniform measure on the unitary circle [9,11]:

$$P^{(N)}(z_n) dz_n = \frac{d\vartheta_n^N}{2\pi}, \quad (4)$$

where dz_n represents the infinitesimal interface's portion around z_n . Hence, we can define the active zone through

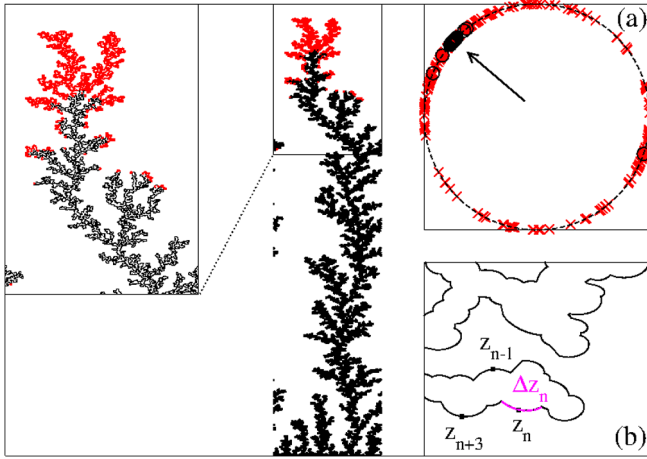


FIG. 2 (color online). Active zone of the DLA. Typical DLA realization obtained through (1) ($\lambda_0 = 10^{-4}$, $L = 1$): black (dark) and red (bright) regions represent the frozen and the active zone. Inset (a): DLA interface on the unitary circle. Red crosses are the boundaries of $\Delta\vartheta_n^N$ for $n \in [N - n_{AZ}, N]$, black circles for $n \ll N - n_{AZ}$: arrow shows where the counterimage of the frozen zone is mostly concentrated. Inset (b): boundary of the DLA showing Δz_n (bright magenta) and the representative point z_n .

the relation $\sum_{n=N-n_{AZ}}^N \frac{\Delta\vartheta_n^N}{2\pi} \geq 0.95$ [Fig. 2, inset (a)]. The scaling of $\langle n_{AZ} \rangle$ is shown in Fig. 3. Now, a well-established fact is that $\mu_{N,n}$ in the active zone exhibits a multifractal scaling [4,10,18]. In this context, growth probability scales differently in different regions characterized by the multifractal exponent α , namely $\mu(\frac{\sqrt{\lambda_0}}{L}) \sim (\frac{\sqrt{\lambda_0}}{L})^\alpha$ ($\alpha_{\min} \leq \alpha \leq \alpha_{\max}$) [18]. Numerical simulations show that α exhibits a stationary dependence on the ratio $(n - N)/\langle n_p \rangle$: $\alpha(\frac{n-N}{\langle n_p \rangle})$ [Ref. [13], Fig. 9 panel (b)]. This relation bridges together multiscaling and multifractality. Indeed, it has been proposed that, although distinct phenomena, multiscaling and multifractality may provide an equivalent description whether $\alpha = \alpha(\frac{r}{R})$, where r and R represent an inner and

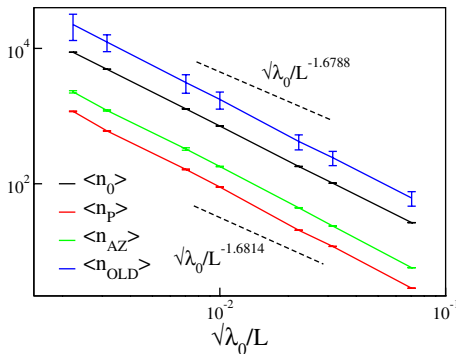


FIG. 3 (color online). Scaling of the characteristic times ruling the DLA growth. Different characteristic times seems to fulfill the scaling law $\sim (\frac{\sqrt{\lambda_0}}{L})^{-D}$, with $D \approx 1.67$ fractal dimension. We took $\langle n_0 \rangle = \frac{4\pi}{\langle \lambda_n \rangle}$ and $L = 1$.

the overall radius of a radial cluster [2]. Since the average radii of the radial deformation of the aggregate scale as $\langle r \rangle \sim e^{2\pi n/\langle n_0 \rangle}$ and $\langle R \rangle \sim e^{2\pi N/\langle n_0 \rangle}$ (Fig. 1 in Ref. [13]), we get $\alpha(\frac{r}{R}) \equiv \alpha(\frac{n-N}{\langle n_p \rangle})$ where $\langle n_p \rangle \sim \langle n_0 \rangle$ (Fig. 3). However, this relationship does not hold for truly radial DLA.

At this point, a question arises: how long does z_n take to pass from the active to the frozen zone? This question is better addressed on the unitary circle. Indeed, when a new bump is created at $\theta_n \simeq \vartheta_n^n$, its size on the unitary circle is approximately $\sqrt{\lambda_n} \simeq \Delta\vartheta_n^N$ [11], with $\langle \Delta\vartheta_n^N \rangle \simeq \sqrt{\frac{4\pi}{\langle n_0 \rangle}}$. When $N > n$, the angle ϑ_n^N changes its position due to Eq. (2), and $\Delta\vartheta_n^N$ shrinks because of the decay of the probability $P^{(N)}(z_n)$ [Eq. (4)]. Eventually, $\Delta\vartheta_n^N$ shrinks to zero (within the machine precision) and the angles ϑ_n^N , counterimages of the points lying in the frozen zone, become indistinguishable on the unitary circle [Fig. 2, inset (a)]. We measured the average time $\langle n_{OLD} \rangle$ for which $\Delta\vartheta_n^{n+n_{OLD}} \simeq 0$ (Fig. 3). Moreover, the fact that the frozen zone almost corresponds to a unique angle on the unitary circle, explains why $|\phi_k^l(e^{i\vartheta_n^k})| \simeq |\phi_k^l(e^{i\vartheta_n^k})| \simeq e^{1/n_p}$ ($k \gg n^{(l)} + n_{AZ} \sim n^{(l)} + n_{OLD}$) and the ensuing conformal invariance, as any $\phi_k(e^{i\theta_n})$ commutes with $\phi_n(e^{i\theta_n})$ leaving unaffected the value of $\Xi^{(N)}(e^{i\theta_n})$ ($N - n_{OLD} \gg k \gg n + n_{OLD}$).

DLA collapse.—So far, we provided a strong evidence of the stationarity of the harmonic measure. The next step is to prove that it is unique and invariant: indeed, estimates of $\mu_{N,n}$ could be strongly affected by fluctuations “and” and “or” memory effects. In general, a sufficient condition for the assessment if a stochastic process has one invariant measure, is the coupling of two realizations of the process with different initial conditions but the same randomness. If one is able to prove that both processes collapse with probability one, this means that there exists a unique invariant measure [19] (see Sec. II in Ref. [13]).

In conformal mapping, the stochastic process is defined by the angles $[\theta_1, \dots, \theta_N]$. Hence, we consider as independent initial conditions $[\theta_1^{(1)}, \dots, \theta_{N_{\text{init}}}^{(1)}]$ and $[\theta_1^{(2)}, \dots, \theta_{N_{\text{init}}}^{(2)}]$ ($N_{\text{init}} \gg \langle n_0 \rangle$), and we extract subsequent angles according to $\theta_N^{(1)} = \theta_N^{(2)}$ ($N > N_{\text{init}}$): collapse arises if and only if (1) $\Delta\vartheta_n^N = (2)\Delta\vartheta_n^N$, $\forall n \in [N - \langle n_{AZ} \rangle, N]$ (Fig. 5 in Ref. [13]). However, this procedure is strongly affected by systematic errors induced by ϕ_n [11,12,20] (Sec. III of Ref. [13]): if a growth attempt is made close to the frozen regions, unphysical particles tend to fill the fjords of the aggregates, leading to clusters’ divergence rather than collapse. Thus, we apply the collapsing procedure to DLA on a lattice.

For DLA on a lattice, randomness is given by the Brownian nature of the upcoming particle’s path: a collapsing protocol may consist on taking the same diffusive trajectories, for particles released from the upper cylinders’ boundaries in both DLA. Therefore, after two initial

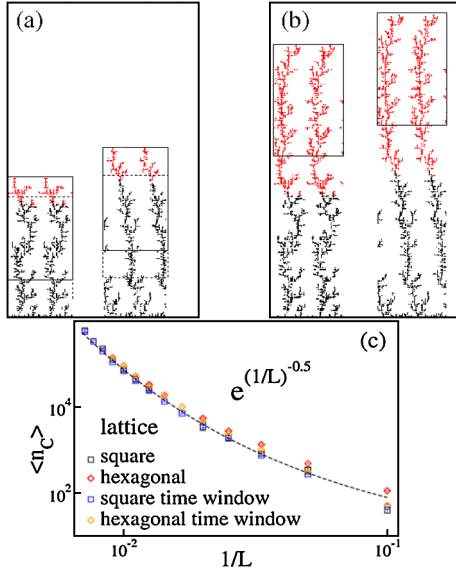


FIG. 4 (color online). DLA collapse. Collapsing protocols for DLA on a lattice (lattice unit = 1). (a) Different initial conditions: two DLA grown independently (black particles); red (bright) particles follow the same Brownian paths on the cylinder surfaces. Frames represent the spatial window ($3L$) within which collapse can arise. (b) Collapsed DLA. (c) Collapsing time $\langle n_C \rangle$ obtained with two different collapsing protocols in both a square (square symbols) and hexagonal lattice (diamonds): spatial window and time window collapse criteria give $e^{(1/L)^{-0.5}}$.

conditions have been built [Fig. 4, panel (a)], protocol is started and it is stopped only when both DLA have collapsed [Fig. 4, panel (b)]; i.e., when they are identical within a window of height $3L$. The average collapsing time $\langle n_C \rangle$ shows a stretched exponential behavior, $\langle n_C \rangle \sim e^{(1/L)^{-0.5}}$, valid in square and in hexagonal lattices [Fig. 4, panel (c)]. The outlined collapsing protocol requires that both DLA are overlapping in a spatial window: we now want that collapse occurs when they are identical within a temporal window $\langle n_{AZ} \rangle$. In this case, DLA collapse is the physical distance between the positions of the last $\langle n_{AZ} \rangle$ homologous particles is zero. Our results strongly indicate that the stretched exponential decay is robust to the change of lattice geometry and definition of collapsing criteria [Fig. 4, panel (c)], but is definitely different from what has been observed for $\langle n_0 \rangle$, $\langle n_P \rangle$, $\langle n_{AZ} \rangle$ and $\langle n_{OLD} \rangle \sim (\sqrt{\lambda_0}/L)^{-D}$ (Fig. 3), that is the average number of particles composing a DLA in a box $L \times L$.

The observed stretched exponential behavior is explained within the conformal mapping framework. The collapsing time n_C can be expressed as $n_C^{-1} \propto \langle p(\{(1)\Delta\vartheta_n^N\})p(\{(2)\Delta\vartheta_n^N\}) \prod_{k=0}^{n_{AZ}} \delta(\{(1)\Delta\vartheta_{N-k}^N - (2)\Delta\vartheta_{N-k}^N\}) \rangle$, where the joint probability distribution $p(\{(1)\Delta\vartheta_n^N\})$ is $p(\{(1)\Delta\vartheta_{N-n_{AZ}}^N, \dots, (1)\Delta\vartheta_N^N\})$, and $\delta(x)$ is the Dirac delta function. Assuming $\Delta\vartheta_n^N$ uncorrelated, we have that $n_C^{-1} \propto \prod_{k=0}^{n_{AZ}} \langle p(\{(1)\Delta\vartheta_{N-k}^N\})^2 \rangle$. Now, taking

$p(\{(1)\Delta\vartheta_{N-k}^N\}) \sim e^{-[(1)\Delta\vartheta_{N-k}^N / \langle (1)\Delta\vartheta_{N-k}^N \rangle]}$, thanks to Eq. (4) we finally obtain $n_C \sim \prod_{k=0}^{n_{AZ}} \langle e^{2(P^{(N)}(z_{N-k})/\mu_{N,N-k})} \rangle \sim \prod_{k=0}^{n_{AZ}} \langle e^{2P^{(N)}(z_{N-k})(\sqrt{\lambda_0}/L)^{-\alpha(k/n_P)}} \rangle$.

Conclusions.—We have shown that the harmonic measure is stationary, unique and invariant on the DLA interface. As a matter of fact, within this comprehensive framework, the system's stationarity entails that multiscaling, multifractality, and conformal invariance appear as a unique emergent property of the growth dynamics. Moreover, the stationarity allows the precise definition of characteristic times, whose scaling exhibit a sole critical exponent: the aggregate's fractal dimension. This is at odds with radial DLAs, for which a stationary phase and an ensuing single scaling exponent cannot be identified, casting very fundamental doubts on the possible existence and definition of a fractal dimension in this geometry. Most important, the uniqueness and invariance of the harmonic measure paves the way for the notion of ergodicity in fractal growth phenomena.

The authors thank F. Martinelli for valuable suggestions. A. T. thanks F. Stenico, E. Mastrostefano, and the Director of the Institute IASI-CNR for granting access to the openMosix cluster HYDRA. A. T. is supported by the Complexity-net pilot project LOCAT.

- [1] T. A. Witten and L. M. Sander, *Phys. Rev. Lett.* **47**, 1400 (1981).
- [2] A. Coniglio and M. Zannetti, *Physica (Amsterdam)* **163A**, 325 (1990).
- [3] C. Amitrano, A. Coniglio, P. Meakin, and M. Zannetti, *Phys. Rev. B* **44**, 4974 (1991).
- [4] T. C. Halsey, P. Meakin, and I. Procaccia, *Phys. Rev. Lett.* **56**, 854 (1986); C. Amitrano, A. Coniglio, and F. di Liberto, *Phys. Rev. Lett.* **57**, 1016 (1986); T. Vicsek, F. Family, and P. Meakin, *Europhys. Lett.* **12**, 217 (1990); B. B. Mandelbrot and C. J. G. Evertsz, *Nature (London)* **348**, 143 (1990).
- [5] H. Kesten, *Stoch. Proc. Appl.* **25**, 165 (1987).
- [6] N. G. Makarov, *Proc. London Math. Soc.* **s3-51**, 369 (1985).
- [7] T. C. Halsey, *Phys. Rev. Lett.* **59**, 2067 (1987).
- [8] P. Meakin, A. Coniglio, H. E. Stanley, and T. A. Witten, *Phys. Rev. A* **34**, 3325 (1986); R. C. Ball and O. R. Spivack, *J. Phys. A* **23**, 5295 (1990); W. G. Hanan and D. M. Heffernan, *Phys. Rev. E* **77**, 011405 (2008); D. A. Adams, L. M. Sander, E. Somfai, and R. M. Ziff, *Europhys. Lett.* **87**, 20001 (2009).
- [9] M. B. Hastings and L. S. Levitov, *Physica (Amsterdam)* **116D**, 244 (1996).
- [10] B. Davidovitch, M. H. Jensen, A. Levermann, J. Mathiesen, and I. Procaccia, *Phys. Rev. Lett.* **87**, 164101 (2001); M. H. Jensen, A. Levermann, J. Mathiesen, and I. Procaccia, *Phys. Rev. E* **65**, 046109 (2002).
- [11] B. Davidovitch, H. G. E. Hentschel, Z. Olami, I. Procaccia, L. M. Sander, and E. Somfai, *Phys. Rev. E* **59**, 1368 (1999).

- [12] A. Taloni, E. Caglioti, V. Loreto, and L. Pietronero, *J. Stat. Mech.* (2006) P09004.
- [13] See Supplemental Material at <http://link.aps.org/supplemental/10.1103/PhysRevLett.109.065501> for (I) the iterated conformal mapping in cylinder geometry, (II) the proof of the existence of the uniqueness of the invariant measure, (III) the collapsing protocol using conformal mappings, and for the figures regarding the stationarity of growth velocity and the scaling of the harmonic measure within the active zone.
- [14] L. Niemeyer, L. Pietronero, and H.J. Wiesmann, *Phys. Rev. Lett.* **52**, 1033 (1984).
- [15] M. Plischke and Z Rácz, *Phys. Rev. Lett.* **53**, 415 (1984).
- [16] P. Meakin, *Fractals, Scaling and Growth Far from Equilibrium* (Cambridge University Press, Cambridge, 1998).
- [17] P. Ossadnik, *Physica (Amsterdam)* **195A**, 319 (1993).
- [18] L. A. Turkevich and H. Scher, *Phys. Rev. Lett.* **55**, 1026 (1985); M. H. Jensen, J. Mathiesen, and I. Procaccia, *Phys. Rev. E* **67**, 042402 (2003).
- [19] F. Martinelli and E. Scoppola, *Commun. Math. Phys.* **120**, 25 (1988).
- [20] M. G. Stepanov and L. S. Levitov, *Phys. Rev. E* **63**, 061102 (2001).